Regional sea level trends due to a Pacific trade wind intensification

Mark A. Merrifield[1] and Mathew E. Maltrud[2]

Received 8 September 2011; accepted 8 October 2011; published 5 November 2011.

[1] Over the past two decades, sea level trends have increased in the western tropical Pacific Ocean with rates that are approximately three times the global average. A general circulation model is used to show that the high rates are caused by a gradual intensification of Pacific trade winds since the early 1990s. The modeled sea level change captures the spatial trend pattern in satellite altimeter sea surface heights and the temporal trend shift in tide gauge observations. In addition to the sea level response, the model is used to show how other aspects of the ocean circulation have increased appreciably in amplitude as a consequence of the trade wind intensification, including tropical surface currents, the shallow meridional over-turning circulation, the Equatorial Undercurrent, and the Indonesian Throughflow. These results highlight an ongoing shift in the state of the tropical Pacific Ocean that will continue as long as the trade wind trend persists. **Citation:** Merrifield, M. A., and M. E. Maltrud (2011), Regional sea level trends due to a Pacific trade wind intensification, *Geophys. Res. Lett.*, *38*, L21605, doi:10.1029/2011GL049576.

1. Introduction

[2] Since the early 1990s, sea level trends obtained from satellite altimetry have been higher in the western tropical Pacific than any other region of the worlds oceans (Figure 1). The 1993–2010 sea level trend pattern features two maxima centered at about 10° north and south of the equator. In situ sea level observations from island tide gauges in the western Pacific indicate that the regional sea level change represents a pronounced shift from near-zero trends between 1950 to the early 1990s to nearly 10 mm yr^{-1} since 1990 [*Merrifield*, 2011] (Figure 1).

[3] Previous modeling studies have shown that wind stress forcing can account for the recent high sea level trends observed in the western tropical Pacific [*Carton et al.*, 2005; *Köhl et al.*, 2007; *Timmermann et al.*, 2010; *Qiu and Chen*, 2010]; however, most of these studies have attributed the high rates to sea level fluctuations associated with El Niño-Southern Oscillation (ENSO) events. The implication is that the recent sea level trends computed over two decades or less largely reflect a tendency toward La Niña conditions over the short analysis period as opposed to a longer-term sea level change. This notion is consistent with the La Niña-like spatial structure of the sea level trends (Figure 1), although the trend pattern extends to higher latitudes in the western tropical Pacific than a typical La Niña event.

[4] A number of studies have reported on an intensification in Pacific trade wind speeds during recent decades [*Liu and Curry*, 2006; *Wentz et al.*, 2007; *Li and Ren*, 2011; *Merrifield*, 2011]. Over the past 50 years, the trade wind intensification has a different temporal character than the dominant climate modes of variability in the Pacific such as ENSO, the Pacific Decadal Oscillation, and the North Pacific Gyre Oscillation [*Merrifield*, 2011; *Li and Ren*, 2011]. The wind increase coincides generally with low frequency changes in sea surface temperature [*Li and Ren*, 2011; *Merrifield*, 2011], latent heat flux [*Yu and Weller*, 2007; *Li et al.*, 2011], outgoing longwave radiation [*Merrifield*, 2011], and precipitation [*Wentz et al.*, 2007] patterns in a manner suggestive of an intensification of the Hadley circulation [*Tanaka et al.*, 2004; *Mitas and Clement*, 2006]. *Fang and Wu* [2008] used a fully coupled ocean-atmosphere general circulation model to show how the intensification pattern can result from global warming forcing, modeled as a zonally uniform heat flux anomaly in the tropics.

[5] Covariations between trade winds and sea level in the tropical Pacific have been examined at decadal [*Lee and McPhaden*, 2008] and interdecadal [*Feng et al.*, 2010] timescales. Although these wind-forced components of satellite altimeter and tide gauge time series have been noted, and the aforementioned modeling studies have demonstrated that wind-forcing can account for recent sea level trend patterns, it has not been fully appreciated that it is the low frequency component of the trade wind-forcing that results in the high rates of sea level rise in the western tropical Pacific over the past 20 years. A modeling study that focuses on the adjustment of the tropical Pacific to low frequency wind-forcing would help to make this dynamical connection.

[6] We use global ocean model simulations to show that sea level adjustments to wind stress trends over a 20-yr time span resemble patterns observed in the satellite altimeter record. Notably, the prominent changes in the tropical Pacific are accounted for in the model and linked to the interdecadal intensification of the trade winds. The results are sensitive to the choice of wind product used to force the model. In addition to the sea level rise pattern in the western tropical Pacific, the model highlights other wind-driven aspects of the tropical Pacific Ocean circulation on these timescales.

2. Methods

[7] The simulations described here were performed using the Parallel Ocean Program (POP) [*Dukowicz and Smith*, 1994] configured to be essentially a stand-alone version of the Community Climate System Model (CCSM3) ocean [*Collins et al.*, 2006]. The POP horizontal grid is defined by a standard Mercator pattern in the southern hemisphere, and a displaced pole grid in the northern hemisphere (with the

[1]Department of Oceanography, University of Hawaii'i at Mānoa, Honolulu, Hawaii, USA.
[2]Fluid Dynamics and Solid Mechanics Group, Los Alamos National Laboratory, Los Alamos, New Mexico, USA.

Copyright 2011 by the American Geophysical Union.
0094-8276/11/2011GL049576

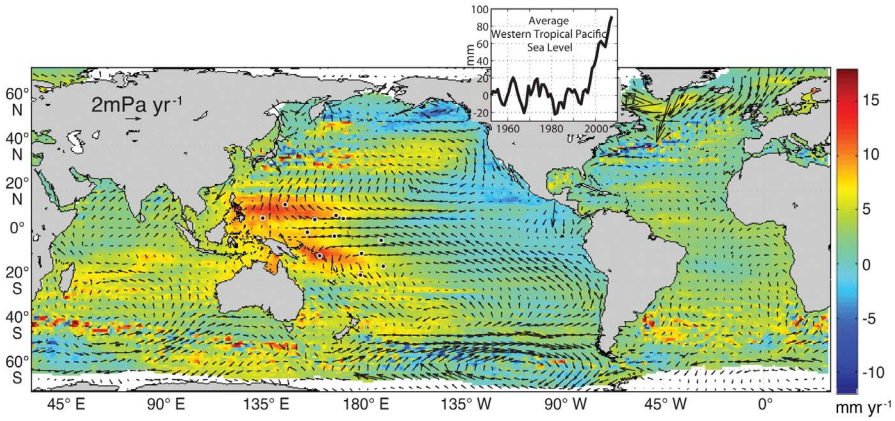

Figure 1. Linear trend (1993-2010) of satellite altimeter SSH showing the region of high rates in the western Tropical Pacific. Vectors denote ECMWF wind stress trends for the same period. The inset is the time series of average sea level obtained from 11 tide gauges [*Merrifield*, 2011] (tide gauge locations denoted by solid dot).

pole in Greenland) to avoid singularities at the North Pole. The longitudinal grid spacing is 1.125° at the equator, while the latitudinal spacing varies smoothly from 0.27° at the equator to just over 0.5° at midlatitudes, then decreases again toward the poles. The relatively high meridional resolution in the tropics is important for realistic simulations of equatorial dynamics. This setup has 40 vertical levels, varying from 10m at the surface to 250m at depth. The model started from rest (with a time step of about 30 minutes) using climatological temperature and salinity fields [*Steele et al.*, 2001] interpolated to this model grid.

[8] Horizontal tracer mixing is calculated using the formulation of *Gent and McWilliams* [1990], and horizontal momentum diffusion using the anisotropic viscosity scheme of *Smith and McWilliams* [2003]. Vertical diffusion coefficients are calculated using the K- Profile Parameterization (KPP) [*Large et al.* [1994], with gravitational instabilities resolved using a large value of 0.1 m^2 s^{-1}. Surface heat, freshwater, and momentum fluxes were calculated using the atmospheric state provided by the Coordinated Ocean-Ice Reference Experiments (CORE) "normal year" climatology [*Large and Yeager*, 2004] averaged to monthly values. This data set was constructed to be "neutral" with respect to El Niño, that is, the seasonal cycle is a long-term average (1958–2000) with the variability chosen from a year (1995) with no strong El Niño or La Niña signal. Thus, the ocean should not display a significant response to these modes. Surface temperature and salinity were restored to observations with a 30-day timescale in regions of climatological sea ice (an explicit sea ice model was not used) and open ocean surface salinity was restored on a one-year scale to control salinity drift.

[9] A control run of 100 years was performed using CORE monthly averaged wind stress, resulting in the upper ocean circulation reaching a near-equilibrium state with the mean and seasonal wind-forcing. From this point, sensitivity experiments were done by varying the applied wind stress but keeping all other model settings the same in order to assess the relationship of changes in wind stress with variations in sea surface height (SSH). We expand on previous studies that have considered the tropical Pacific Ocean response to daily [*Timmermann et al.*, 2010] and monthly [*Qiu and Chen*, 2010] wind-forcing by considering the response to an interdecadal wind change, modeled here as a linear trend in wind stress imposed on the climatological forcing over a 20-yr span. The spatial pattern of the wind stress trend is calculated from both the European Centre for Medium-Range Weather Forecasts (ECMWF) operational ocean analysis/reanalysis system (ORA-S3) [*Balmaseda et al.*, 2008] (named "ET" for "ECMWF Trend") and NCAR/NCEP [*Kalnay et al.*, 1996] (named "NT" for "NCEP Trend") reanalyses by performing a linear regression on annual means for 1993–2009 at each grid point (Figure 1). The trend patterns correspond to a general intensification of the mean atmospheric circulation in the tropical and subtropical Pacific. Because the model annual mean time series considered here exhibit linear changes over the period of trending winds, a difference in annual averages between a given year and the control year provides a robust estimate of the linear trend for all variables considered.

3. Results

[10] The simulated SSH trends from run ET (Figure 2a) bear a striking resemblance to the satellite altimeter SSH trends (Figure 1) throughout the Pacific basin. In particular, the model reproduces the spatial SSH trend pattern in the western tropical Pacific with maxima north and south of the equator, which is quantitatively reflected by a spatial correlation of 0.8 of the fields in the tropical Pacific. When the model trend is subtracted from the altimeter trend (Figure 2b), the western Pacific maxima are greatly reduced, implying that the model captures the primary forcing mechanism responsible for the large *SSH* trend, which is the slowly intensifying trade winds over a nearly 20-yr span as opposed to shorter period wind fluctuations. The increasing easterly winds near the equator balance zonal SSH gradients, and negative wind stress curl anomalies off the equator lead to wind-driven convergences of water in the upper ocean, which tend to propagate westward as positive SSH anomaly Rossby waves.

[11] The model results indicate that the western Pacific SSH rise pattern is due to a wind-driven convergence of water in the upper ocean, as opposed to a change in ocean density driven by surface buoyancy fluxes. Because POP is a Boussinesq model, SSH changes due to density changes

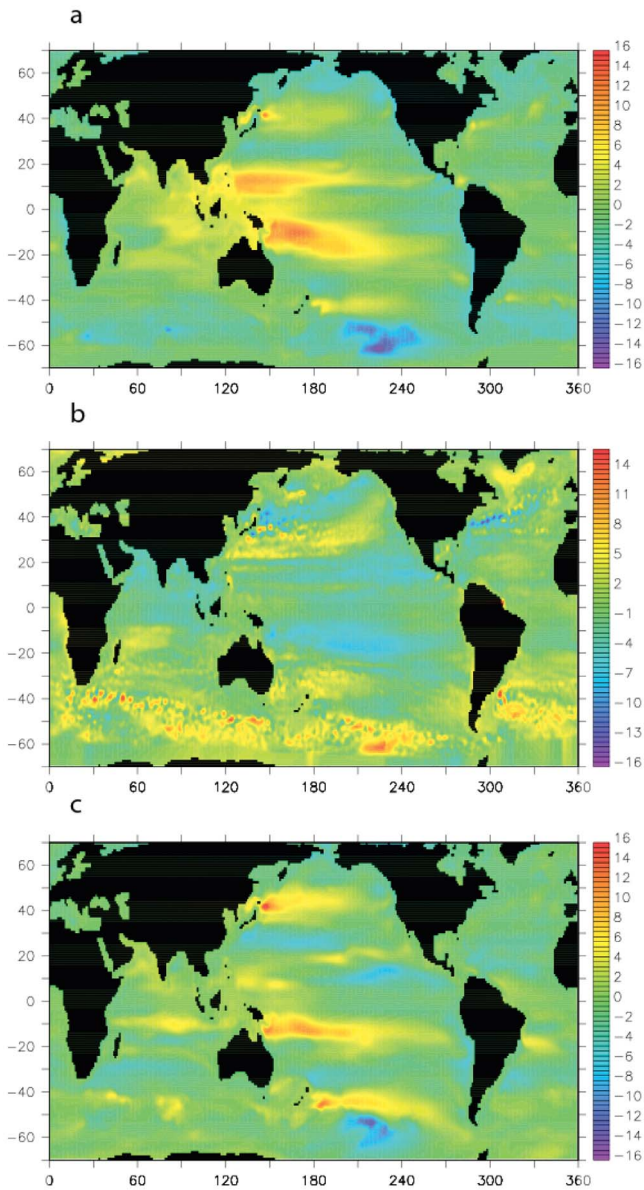

Figure 2. (a) 20-yr SSH trend (mm yr^{-1}) for run ET. (b) Difference between the run ET trend (Figure 2a) and altimeter trend (Figure 1). (c) 20-yr SSH trend for run NT.

are not included explicitly, although they can be inferred from the model density anomalies. The model does include a time dependent surface heat flux component because of the mismatch between the surface heat flux climatology and the imposed wind stress trend; however, we estimate this response to be small.

[12] Mismatches between the model and observed SSH trends exist, particularly at mid to high latitudes (Figure 2b). The discrepancies may be due to errors in the wind product or the neglect of surface heat and freshwater forcings. In addition, a full specification of the fluctuating wind-forcing is likely to be more important for simulating observed sea level trends at higher latitudes than near the equator. Rossby wave adjustments to wind variations are slower at higher latitude, which is likely to have an appreciable influence on SSH trend patterns estimated over 20 years spans. The use of a trending wind stress ignores these effects.

[13] Similar to previous theoretical and numerical modeling studies (discussed by *Cane et al.* [1997] and *Fang and Wu* [2008]), the trending trade winds result in other notable changes in the tropical circulation besides the SSH trend. In the POP simulation increased trade winds accelerate the North and South Equatorial Currents, contributing to the mass convergence in the western tropical Pacific. Some of this water returns to the east in a stronger North Equatorial Countercurrent, which together with the North Equatorial Current defines a spin-up of the tropical gyre [*Qiu and Chen*, 2010] (Figure 3a).

[14] The trade wind intensification also leads to a strengthening of the Equatorial Undercurrent (an increase from 29 Sv to 37 Sv at 140W, Figure 3b) and additional transport to the Indian Ocean via the Indonesian Throughflow (~2 Sv increase, Figure 3c), both of which appear to be reflected in observations. Current measurements exhibit a rise in the undercurrent speed at the equator between the mid-1990s and early 2000s which [*Cheng et al.*, 2007] show results in a 6 Sv increase in transport at 140W. Estimates of changes in Indonesian Throughflow transport are more uncertain, but a 2 Sv increase is not inconsistent with values reported by *Sprintall et al.* [2009] using *in-situ* data and *Feng et al.* [2010] using sea level measurements. Temperature increases in Figures 3a and 3b are due to a deepening of the equatorial thermocline. An increase in poleward Ekman transport at the surface is compensated by an increase in equatorward geostrophic transport, resulting in an enhancement of the shallow overturning cells in the Pacific (Figure 3d) [*McPhaden and Zhang*, 2002, 2004; *Lee and McPhaden*, 2008; *Cheng et al.*, 2007]. The shoaling of the undercurrent and the spin-up of the overturning cells contribute to enhanced upwelling in the equatorial cold tongue region of the eastern tropical Pacific.

[15] ECMWF is only one of the possible wind stress products one could use to test the trade wind spin-up hypothesis. Indeed, since the control run was performed using the NCAR/NCEP-based CORE forcing, it makes sense to also test the NCEP product in a similar way as was done for ECMWF. Figure 2c shows the SSH trend from run NT where the only difference from run ET is the use of the NCEP trend superimposed on the seasonal wind stress climatology instead of the ECMWF trend. While there is still a hint of the SSH trend pattern seen in the altimeter SSH data (Figure 1), the rates are much weaker, particularly north of the equator, and the spatial correlation of observed and modeled rates in the tropical Pacific drops to 0.5 compared to 0.8 for run ET.

[16] Given the different responses from the two wind stress products, it is important to determine which is more realistic. Besides using distinct numerical models for the calculations, one significant characteristic of the ECMWF reanalysis is that it assimilates scatterometer winds [*Uppala et al.*, 2005] while this version of NCEP does not. To assess the importance of the scatterometer winds, we use a data set that blends NCEP with QuikSCAT scatterometer winds for the years 2000–2008 [*Milliff et al.*, 1999] (data available at http://dss.ucar.edu/datasets/ds744.4). Figure 4 shows the trend in the zonal wind stress in each of the products. The merged case (Figure 4c) appears to nudge the NCEP trend toward the ECMWF pattern in the western tropical Pacific due to the inclusion of the scatterometer data. In particular, the trend averaged over 5°N to 10°N (Figure 4d) shows that

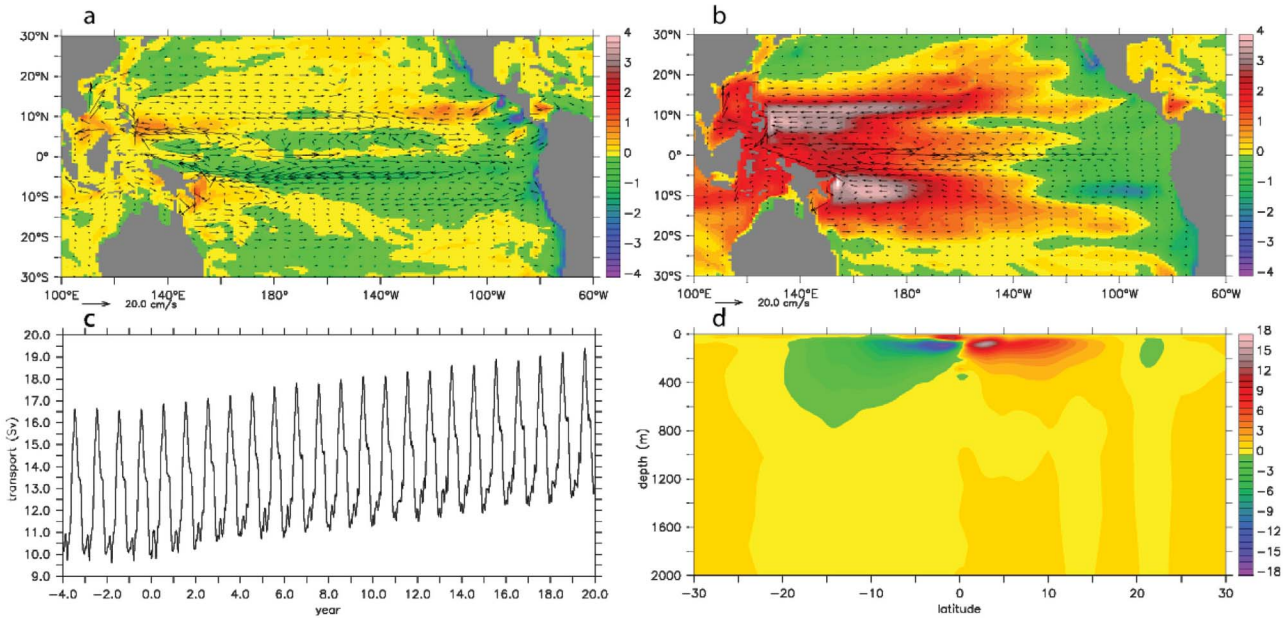

Figure 3. (a) Difference in upper 50m average temperature (°C) and velocity between year 20 of run ET and the final year of the control run. (b) Difference in 50m to 250m average temperature (°C) and velocity between year 20 of run ET and the final year of the control run. (c) Volume transport through the Indonesian Throughflow for the final 4 years of the control run (years −4 to 0) and run ET (years 0 to 20). (d) Difference in meridional overturning transport stream function (Sverdrups) between year 20 of run ET and the final year of the control run. Positive values indicate clockwise flow.

the merged case lies between the NCEP and ECMWF curves between 160°E and 160°W, implying a significantly stronger increase in the trade winds in this region. This is particularly significant since the northern hemisphere is also where the SSH trend disagrees the most in the two simulations. In addition, the spatial correlation of the ECMWF and NCEP+QuikSCAT trends (r = 0.7) is greater than that of the NCEP and NCEP+QuikSCAT trends (r = 0.6) over the tropical Pacific. If one hypothesizes that the inclusion of scatterometer measurements (whether via assimilation or blending) results in a more realistic depiction of the wind, then this implies that the ECMWF trend is likely to be more realistic in this region than NCEP. Thus we may have more confidence in the ocean model's response to the ECMWF

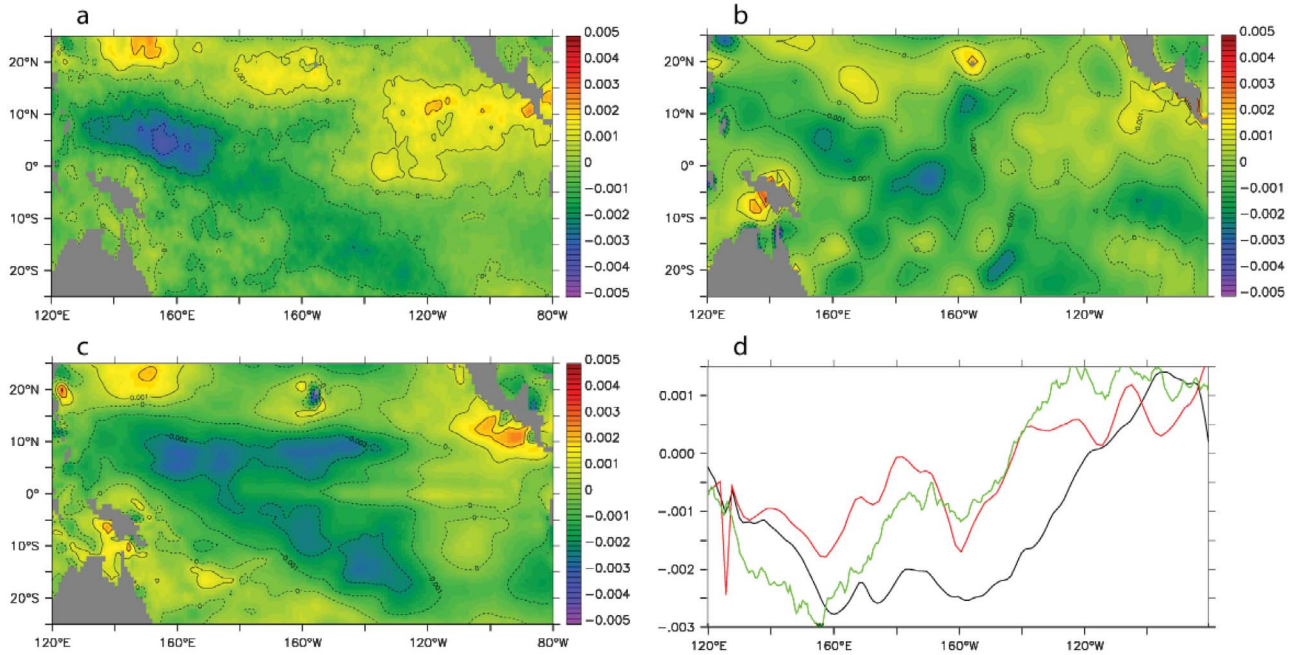

Figure 4. Trend in annual average zonal wind stress (Pa yr^{-1}) for the years 2000-2008 for (a) ECMWF, (b) NCEP, and (c) NCEP blended with QuikSCAT. (d) Trend in annual mean zonal wind stress averaged over 5°N to 10°N for ECMWF (black curve), NCEP (red), and blended (green).

product. A number of recent studies have noted improved model performance when using scatterometer winds compared to reanalysis products without scatterometer winds [e.g., *Agarwal et al.*, 2007; *Jiang et al.*, 2008].

4. Discussion

[17] These results add further confirmation that sea level changes in the western tropical Pacific are indicative of a multidecadal increase in the Pacific trade winds, similar to but distinct from wind-driven La Niña events on shorter timescales. Reports of Pacific trade wind trends in recent decades describe the increase as starting prior to the 1990s [*Li et al.*, 2011; *Li and Ren*, 2011; *Yu and Weller*, 2007]; however, western tropical Pacific sea level variations suggest that the wind change is prominent and persistent after 1990 [*Merrifield*, 2011]. This is the only occurrence of a prolonged western tropical Pacific sea level rise/trade wind enhancement on these timescales in the available tide gauge records dating back to the mid-20th century. As such outlooks for when this wind pattern is likely to abate are uncertain.

[18] Because the trade wind increase tracks various measures of regional and global warming [*Merrifield*, 2011], and given numerical simulations that have linked the trade wind increase with global warming forcing [*Fang and Wu*, 2008], it seems plausible that the Pacific trade wind intensification, and perhaps aspects of the Hadley circulation as a whole, may be the signature of a forced response to warming rather than a natural climate variation. This scenario implies that the trade winds may continue to track heat increases unless other processes begin to override the tendency. Further research is needed to understand the driving mechanism of the trade wind intensification. While it is in effect, sea level and ocean circulation trends in the tropical Pacific will continue.

[19] **Acknowledgments.** The altimeter SSH products were produced by Ssalto/Duacs and distributed by AVISO, with support from the Centre National d'Etudes Spatiales (CNES). Thanks to R. Milliff for help with scatterometer winds. M. Merrifield was supported by the Office of Climate Observations, NOAA (NA17RJ1230). M. Maltrud was supported by the Department of Energy Office of Science, Biological and Environmental Research.

[20] The Editor thanks two anonymous reviewers for their assistance in evaluating this paper.

References

Agarwal, N., R. Sharma, S. K. Basu, A. Sarkar, and V. K. Agarwal (2007), Evaluation of relative performance of QuikSCAT and NCEP re-analysis winds through simulations by an OGCM, *Deep Sea Res., Part I*, *54*, 1311–1328.

Balmaseda, M. A., A. Vidard, and D. L. Anderson (2008), The ECMWF Ocean Analysis System: ORA-S3, *Mon. Weather Rev.*, *136*, 3018–3034.

Cane, M. A., A. C. Clement, A. Kaplan, Y. Kushnir, D. Pozdnyakov, R. Seager, S. E. Zebiak, and R. Murtugudde (1997), Twentieth-century sea surface temperature trends, *Science*, *275*, 957–960, doi:10.1126/science.275.5302.957.

Carton, J. A., B. S. Giese, and S. A. Grodsky (2005), Sea level rise and the warming of the oceans in the Simple Ocean Data Assimilation (SODA) ocean reanalysis, *J. Geophys. Res.*, *110*, C09006, doi:10.1029/2004JC002817.

Cheng, W., M. J. McPhaden, D. Zhang, and E. J. Metzger (2007), Recent changes in the Pacific subtropical cells inferred from an eddy-resolving ocean circulation model, *J. Phys. Oceanogr.*, *37*, 1340–1356, doi:10.1175/JPO3051.1.

Collins, W. D., et al. (2006), The Community Climate System Model version 3 (CCSM3), *J. Clim.*, *19*, 2122–2143, doi:10.1175/JCLI3761.1.

Dukowicz, J. K., and R. D. Smith (1994), Implicit free-surface method for the Bryan-Cox-Semtner ocean model, *J. Geophys. Res.*, *99*, 7991–8014.

Fang, C., and L. Wu (2008), The role of ocean dynamics in tropical Pacific SST response to warm climate in a fully coupled GCM, *Geophys. Res. Lett.*, *35*, L08703, doi:10.1029/2007GL033097.

Feng, M., M. J. McPhaden, and T. Lee (2010), Decadal variability of the Pacific subtropical cells and their influence on the southeast Indian Ocean, *Geophys. Res. Lett.*, *37*, L09606, doi:10.1029/2010GL042796.

Gent, P. R., and J. C. McWilliams (1990), Isopycnal mixing in ocean circulation models, *J. Phys. Oceanogr.*, *20*, 150–155.

Jiang, C., L. Thompson, and K. A. Kelly (2008), Equatorial influence of QuikSCAT winds in an isopycnal ocean model compared to NCEP2 winds, *Ocean Modell.*, *24*, 65–71.

Kalnay, E., et al. (1996), The NCEP/NCAR 40-year reanalysis project, *Bull. Am. Meteorol. Soc.*, *77*, 437–471.

Köhl, A., D. Stammer, and B. Cornuelle (2007), Interannual to decadal changes in the ECCO Global Synthesis, *J. Phys. Oceanogr.*, *37*, 313–337.

Large, W. G., and S. G. Yeager (2004), Diurnal to decadal global forcing for ocean and sea-ice models: The data sets and flux climatologies, *Tech. Note 460+STR*, Natl. Cent. for Atmos. Res., Boulder Colo.

Large, W. G., J. C. McWilliams, and S. C. Doney (1994), Oceanic vertical mixing: Review and a model with a nonlocal boundary layer parameterization, *Rev. Geophys.*, *32*, 363–403.

Lee, T., and M. J. McPhaden (2008), Decadal phase change in large-scale sea level and winds in the Indo-Pacific region at the end of the 20th century, *Geophys. Res. Lett.*, *35*, L01605, doi:10.1029/2007GL032419.

Li, G., and B. Ren (2011), Evidence for strengthening of the tropical Pacific Ocean surface wind speed during 1979–2001, *Theor. Appl. Climatol.*, doi:10.1007/s00704-011-0463-3, in press.

Li, G., B. Ren, C. Yang, and J. Zheng (2011), Revisiting the trend of the tropical and subtropical Pacific surface latent heat flux during 1977–2006, *J. Geophys. Res.*, *116*, D10115, doi:10.1029/2010JD015444.

Liu, J., and J. A. Curry (2006), Variability of the tropical and subtropical ocean surface heat flux during 1989–2000, *Geophys. Res. Lett.*, L05706, doi:10.1029/2005GL024809.

McPhaden, M. J., and D. Zhang (2002), Slowdown of the meridional overturning circulation in the upper Pacific Ocean, *Nature*, *415*, 603–608.

McPhaden, M. J., and D. Zhang (2004), Pacific Ocean circulation rebounds, *Geophys. Res. Lett.*, *31*, L18301, doi:10.1029/2004GL020727.

Merrifield, M. A. (2011), A shift in western tropical Pacific sea-level trends during the 1990s, *J. Clim.*, *24*, 4126–4138, doi:10.1175/2011JCLI3932.1.

Milliff, R. F., W. G. Large, J. Morzel, G. Danabasoglu, and T. M. Chin (1999), Ocean general circulation model sensitivity to forcing from scatterometer winds, *J. Geophys. Res.*, *104*(C5), 11,337–11,358, doi:10.1029/1998JC900045.

Mitas, C. M., and A. Clement (2006), Recent behavior of the Hadley cell and tropical thermodynamics in climate models and reanalyses, *Geophys. Res. Lett.*, *33*, L01810, doi:10.1029/2005GL024406.

Qiu, B., and S. Chen (2010), Interannual-to-decadal variability in the bifurcation of the North Equatorial Current off the Philippines, *J. Phys. Oceanogr.*, *40*, 2525–2538.

Smith, R. D., and J. C. McWilliams (2003), Anisotropic horizontal viscosity for ocean models, *Ocean Modell.*, *5*, 129–156.

Sprintall, J., S. E. Wijffels, R. Molcard, and I. Jaya (2009), Direct estimates of the Indonesian Throughflow entering the Indian Ocean: 2004–2006, *J. Geophys. Res.*, *114*, C07001, doi:10.1029/2008JC005257.

Steele, M., R. Morley, and W. Ermold (2001), PHC: A global ocean hydrography with a high quality Arctic Ocean, *J. Clim.*, *14*, 2079–2087.

Tanaka, H. L., N. Ishizaki, and A. Kitoh (2004), Trend and interannual variability of Walker, monsoon and Hadley circulations defined by velocity potential in the upper troposphere, *Tellus, Ser. A*, *56*, 250–269.

Timmermann, A., S. McGregor, and F.-F. Jin (2010), Wind effects on past and future regional sea-level trends in the southern Indo-Pacific, *J. Clim.*, *23*, 4429–4437.

Uppala, S. M., et al. (2005), The ERA-40 re-analysis, *Q. J. R. Meterorol. Soc.*, *131*, 2961–3012.

Wentz, F. J., L. Ricciardulli, K. Hilburn, and C. Mears (2007), How much more rain will global warming bring?, *Science*, *317*, 233–235.

Yu, L., and R. A. Weller (2007), Objectively analyzed air-sea heat fluxes for the global ice-free oceans (1981-2005), *Bull. Am. Meteorol. Soc.*, *88*, 527–539, doi:10.1175/BAMS-88-4-527.

M. E. Maltrud, Fluid Dynamics and Solid Mechanics Group, Los Alamos National Laboratory, Los Alamos, NM 87545, USA. (maltrud@lanl.gov)

M. A. Merrifield, Department of Oceanography, University of Hawaii'i at Mānoa, 1000 Pope Rd., MSB 317, Honolulu, HI 96822, USA. (markm@soest.hawaii.edu)